Silicon (2022) 14:7933–7938
https://doi.org/10.1007/s12633-021-01570-x

ORIGINAL PAPER

TFET Biosensor Simulation and Analysis for Various Biomolecules

P. Vimala[1] · L. Likith Krishna[1] · S. S. Sharma[1]

Received: 7 September 2021 / Accepted: 23 November 2021 / Published online: 19 January 2022

Abstract
This paper investigates the simulation and performance of Tunnel field effect transistor (TFET) with a nanocavity in it, which can be used for bio sensing application. The entire simulation is done using the tool Silvaco Atlas TCAD. This paper mainly aims in comparing the different parameters for few biomolecules which has different dielectric constant values, namely Streptavidin, Biotin, APTES, Cellulose and DNA. The device structure here consists of a nanocavity near the source end, which is used to place these biomolecules and hence observe the variation of the Drain current v/s Gate voltage characteristic graph, these biomolecules that are having unique dielectric constants are placed within this cavity and these graphs are observed. The energy band diagram of this device is obtained; on top of this various other parameters namely Surface Potential, Electric field are observed for the above-mentioned Biomolecules. The Length of the cavity of the biosensor is also varied to observe the difference, in addition to this Ion (ON current) variation is plotted for the change in the dielectric constant of the biomolecule.

Keywords TFET · Nanocavity · Drain current · Gate Voltage · Biomolecules · Bio sensing · ON current

1 Introduction

Biological monitoring and the processes involving biochemical substances are important for medical applications. Biosensors that are highly sensitive, cost-effective, and very specific are in demand since they put up to the realization of extremely accurate diagnosis of certain medicines. Hence, various biosensors have been studied extensively because of inception of first-generation biosensors that utilized glucose oxidase during 1962 [1]. A Biosensor is an analytical device that produces electrical signals by detecting changes in biological processes. The basic working principle of the FET biosensor is the modulation of the bands due to the change in the effective coupling between the gate and the channel, owing to the change in the dielectric constant of the immobilized biomolecule present in the nanogap cavity [2].

A biological process is a term which can be any of the following biological element or material like enzymes, tissues, microorganisms or cells. Biosensors that are based on FETs are in popular use because of their excellence in label-free electrical detection, ultra-sensitivity, very less production cost and, mass manufacturing ability. The flow of current is controlled by electric field in FETs [3, 4]. FET based biosensors are used to detect biological species owing to miniaturization, cost-effectiveness, and label-free detection [5]. When the nanogaps are occupied by the neutral/charged biomolecules, they alter the oxide capacitance resulting in the change in drain current and threshold voltage [6]. The sensing mechanism of the targeted biomolecule mainly consists of two different stages such as detection of the bio- molecules and transduction. The detection stage carried out by analyzing the targeted biomolecules and in the transduction stage coverts this physiochemical reaction into measurable electrical which can be further processed [7].

Biosensors that were based on FETs were utilized as Ion Sensitive Field Effect Transistor (ISFET) in the beginning. The diagnosis of neutral biomolecules that was difficult for ISFET was succeeded by using Impact Ionization Junction less FET (JFET) along with MOSFET (IMOS) which became the other novel device technologies reported for biosensing applications [8–10]. These devices suffered from various issues like very high off-state leakage current, low drive current, random dopant fluctuations which was highly complex when it came to fabrication. In IMOS, current was injected in the presence of a high intensity of electric filed in

✉ P. Vimala
ervimala@gmail.com

[1] Department of ECE, Dayananda Sagar College of Engineering, Bengaluru, India

to drain end. This process requires a higher drain to source bias voltage. In addition to this, the manufacturing of this device is extremely complex which is under sub-40 nm gate length [11–13]. Consequently, Impact Ionization MOSFET was disregarded for low-power and ultra-sensitive biosensors. Junction FET suffered adversely because it is based on reverse-biased semiconductor junction and therefore has some gate leakage current due to the presence of minority charge carriers [14–16]. This resulted in static power dissipation and low- sensitivity of JFET and affected its application in biosensors [17, 18]. One of the most important and crucial step in DM-TFET process step is to carve the nanogap cavity which is usually done by selective wet etching [19]. To detect targeted biomolecules the oxide layer of the FET is employed with the bio receptors/bio-recognition element. Once these receptors captured the targeted biomolecules, they have under- gone conjugation process which generates electrochemical re- actions and these electrochemical reactions lead to the gating effect of the semiconductor device [20, 21].

This paper focuses on finding the impact of introducing materials with different dielectrics namely Steptavidin, Biotin, Aminopropyltriethoxysilane (APTES), Cellulose, and Deoxyribonucleic acid (DNA), and observing its I-V characteristics. The presence of biomolecules is characterized by the change in dielectric constants and the associated charge densities, which, in turn, modulates the Schottky barrier (SB) width at the source-channel (metal/Si) junction, owing to the formation of an electron-CP in an undoped-Si film [22]. From carefully analyzing the simulation results, we can infer that TFET is suitable for biosensing applications. The device simulation is carried out in Silvaco ATLAS TCAD, and the graphs are also plotted with the same tool, along with this MATLAB from Math Works is used to plot few graphs.

2 Device Structure

Figure 1 shows the structure of the proposed device which is Tunnel field Effect Transistor (TFET) with a Nano cavity used for biosensing application. It consists of four main regions namely Source, Drain, and Channel which is yellow, and oxide region that is indicated by blue color. Along with this, it consists of two gate electrodes, a source, and a drain electrode each of which is indicated by a thin blue line that can be observed in the figure. The major difference observed here in this structure when compared to the TFET structure is the nanocavity region which is indicated by the red color. Here nanocavity plays an important role in which the molecules with different dielectrics are placed. The source and drain are 25 nm each, and the length of nanocavity is

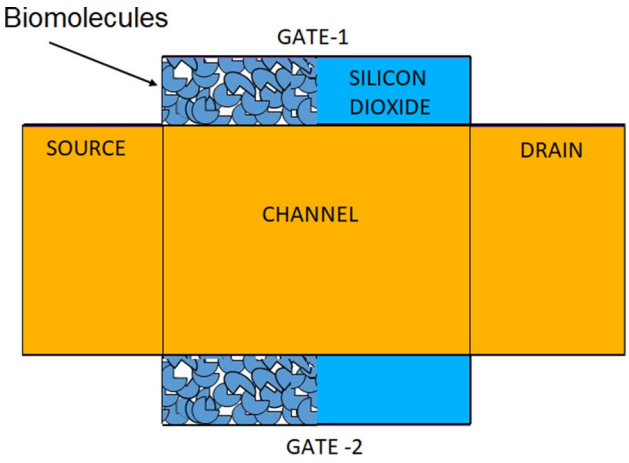

Fig. 1 TFET structure with nanocavity

Table 1 Parameters, Symbols and Its values used in Simulation

Sl. No	Parameter	Symbol	Values
1	Length of Source	L_s	25 nm
2	Length of cavity	L_c	25 nm
3	Length of Drain	L_D	0.75 nm
4	Length of Gate	L_G	50 nm
5	Work Function of Gate Material	ϕ_G	4.2 eV
6	Work Function of Source and Drain	ϕ_S, ϕ_D	4.2 eV
7	Doping Concentration of Source (N-type)	N_S	$1\times10^{20}/cm^3$
8	Doping Concentration of Drain (N-type)	N_D	$1\times10^{16}/cm^3$
9	Doping Concentration of Channel (N-type)	N_{CH}	$5\times10^{18}/cm^3$

25 nm, the overall channel length is 50 nm. Table 1 listed the parameters and its value used for simulation.

3 Results and Discussion

Figure 2 indicates energy band diagram with respect to various biomolecules of Biosensor of this proposed device structure for biomolecules having various dielectric constants shown in Table 2. Electrons need the energy to jump from a lower energy level to a higher energy level. The dotted lines in the graph indicate the valence band and solid lines indicate the conduction band. The bandgap before tunneling is approximately 1 eV. During tunneling, different energy levels in valance and conduction band can be observed for different biomolecules.

Figure 3 indicates variation of Potential for various dielectric values, when Vds = 1 V and Vgs = 0.5 V. Potential

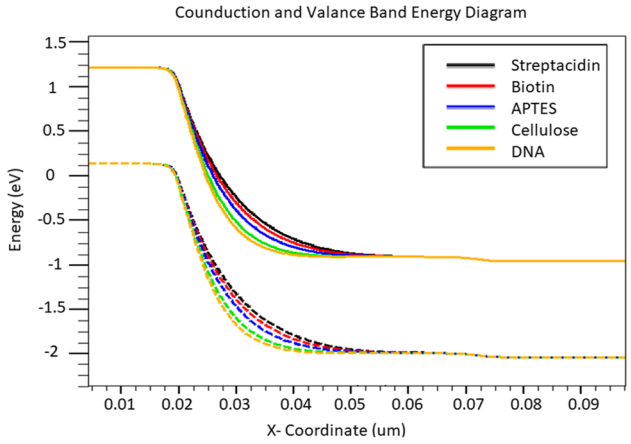

Fig. 2 Energy band diagram with respect to various biomolecules of Biosensor

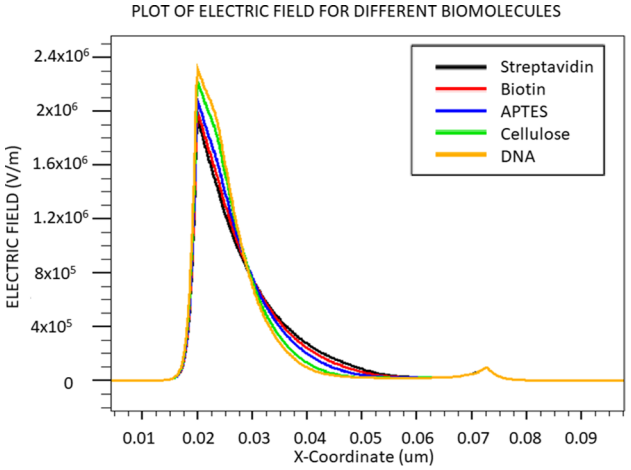

Fig. 4 Plot of Electric field of TFET Biosensor for different biomolecules

Table 2 Biomolecules with their Dielectric Values

Sl. No	Biomolecules	Dielectric Constant
1	DNA	8.7
2	Cellulose	6.1
3	APTES	3.57
4	Biotin	2.63
5	Streptavidin	2.1

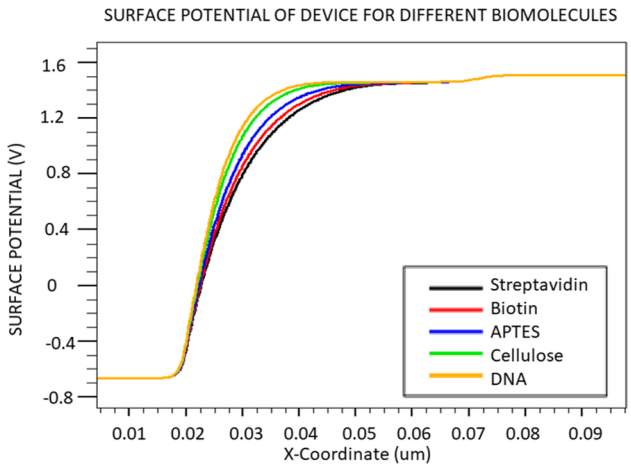

Fig. 3 Plot of Surface potential of TFET Biosensor for various biomolecules

is minimum at the Source region and starts increasing across the channel and further increases in the Drain region. The potential starts from -0.64 V and saturates at 1.51 V. For different values of dielectric constant, the potential of the device changes. From the graph, we can observe that the steep and high potential is obtained for a greater value of the dielectric constant.

Figure 4 indicates variation of Electric Field across channel of this device with Vds = 1 V and Vgs = 0.5 V. In the graph, we can observe two peaks since we have two gates for our device structure. At each point, the electric field is measured, and the sharp points denote the junction. For DNA having the dielectric constant K = 8.7, the electric field is 2.28×10^6 and 1.0×10^5. For Cellulose having dielectric constant K = 6.1, the electric field is 2.16×10^6 and 1.0×10^5. For APTES having the dielectric constant K = 3.57, the electric field is 1.97×10^6 and 1.0×10^5. For Biotin having the dielectric constant K = 2.63, the electric field is 1.87×10^6 and 1.0×10^5. For Streptavidin having the dielectric constant K = 2.1, the electric field is 1.8×10^6 and 1.0×10^5. For different values of dielectric constant, the electric field across the device changes. The electric field is directly proportional to the dielectric value and from the graph, we can observe that as we increase the value of dielectric constant the electric field across the device increases. This is because, when biomolecules are immobilized in the nano-cavity region, the dielectric modulation effect modulates the work function.

Figure 5 indicates plot of I-V Characteristics for different values of dielectric constants by plotting the drain current (I_D) in linear on the left of Y-axis, Gate voltage (V_G) in Volts on the X- axis. This voltage is varied in the steps of 0.05 V. The channel length is kept constant at 50 nm. From the figure, we observe that drain current increases as gate voltage increases from 0.1 V to 1 V. For Streptavidin having the dielectric constant, K = 2.1 the value of I_d starts increasing from 0.9 V. For biotin having the dielectric constant K = 2.63 the value of I_d starts increasing from 0.75 V. For APTES having the dielectric constant of K = 3.57 the value of I_d starts increasing from 0.55 V and saturates at drain

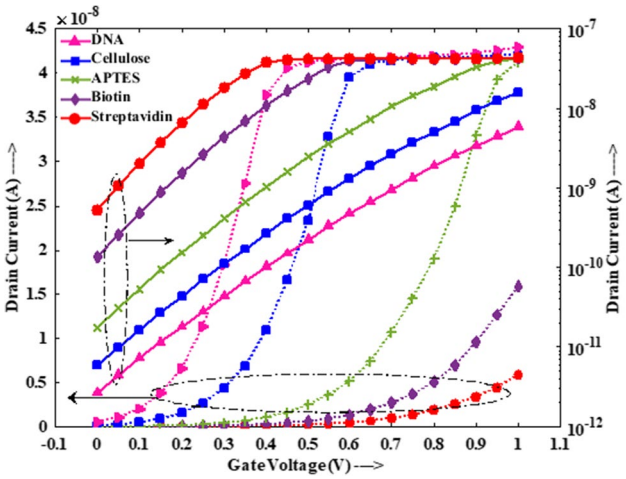

Fig. 5 ID v/s VG plot for different Biomolecules

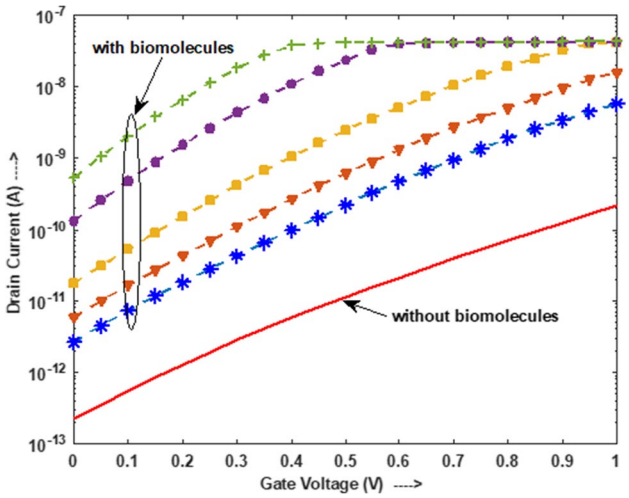

Fig.6 Effect of with and without biomolecule on drain current

current 4×10^{8}A and 1 V. For Cellulose having a dielectric constant of K = 6.1 the value of I_d starts increasing from 0.3 V and saturates at drain current 4×10^{-8}A and 1v. For DNA having the dielectric constant of K = 8.7 the value of I_d starts increasing from 0.15 V and saturates at drain current 4×10^{-8}A and 1 V. Also, the figure shows the plot of I-V Characteristics for different values of dielectric constants by plotting the drain current (I_d) in logarithmic on the right of Y-axis, gate voltage (Vg) in Volts on the X-axis. The voltage is varied in the steps of 0.05 V. The channel length is kept constant at 50 nm. The Y-axis is in the logarithmic scale. For Dielectric constant K = 2.1 I_d is in the range of 10^{-12}A and saturates at the range of 10^{-7}A, similar characteristics are observed for all the materials with different dielectric values. All of these drain current values saturate at the range of 10^{-7} A as shown in the figure.

Figure 6 shows the analysis of drain current with and without the presence of biomolecules. The lower drain current attains when air as a dielectric value that is without biomolecule represented as solid line in the figure. When there is the presence of biomolecules causes a considerable increase in drain current due to a reduction in tunnelling barrier width shown in dotted lines. Different biomolecules like DNA, Cellulose, APTES, Biotin and Streptavidin are considered for this analysis and used different markers in the figure.

Figure 7 indicates the plot of I-V Characteristics for different values of cavity lengths by plotting the drain current (I_d) in Amperes on the Y-axis, gate voltage (Vg) in Volts on the X- axis. The cavity length is increased in the steps of 5 nm. We have taken APTES Biomolecule of dielectric constant K = 3.5, which is a medium range of dielectric value. From the graph, we can observe that the value of I_d starts increasing from 0.55 V and saturates at drain current 4×10^{08}A and 1 V. The graph illustrates that increasing cavity length does not result in a substantial change in driving current. As a result, we may conclude that changing the cavity length for different cavity thicknesses has no influence on the drain current [6, 23].

Figure 8 shows the influence of I_{ON} current on this proposed device structure for distinct values of various dielectric constants. Inferring the above figure, we discover the raise in dielectric constant considerably raises the ON current. This is because an increase in k causes the electric current at the tunnel junction to increase, resulting in a reduction in tunnel width.

Figure 9 indicates the variation of Sensitivity with respect to Dielectric Constant (K) where Sensitivity is plotted along the Y-axis and Dielectric Constant of the biomolecules is represented along the X-axis. The figure clearly shows that for smaller values of Dielectric constant, the sensitivity is

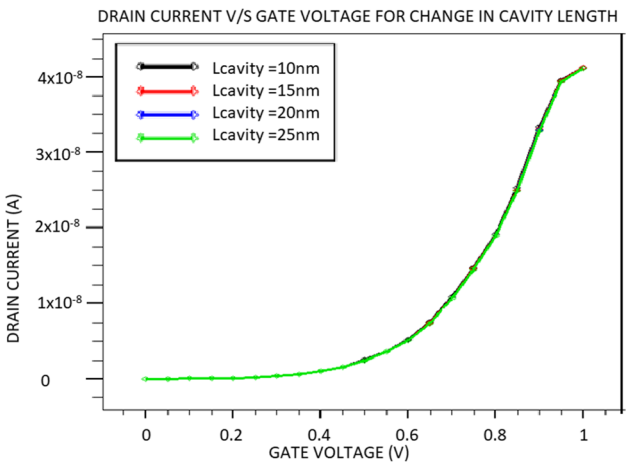

Fig. 7 ID v/s VG for change in Length of cavity

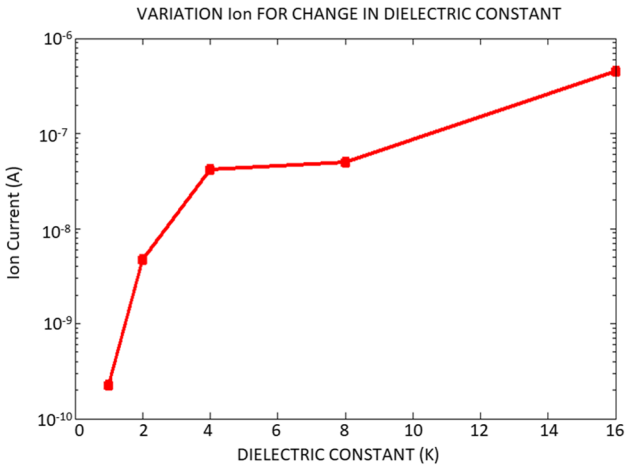

Fig. 8 ON current plot for change in Biomolecules with different dielectric values

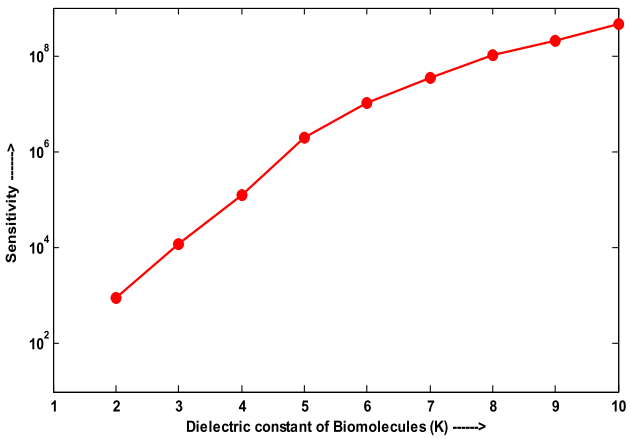

Fig. 9 Sensitivity vs Dielectric Constant of Biomolecules

lower, and the sensitivity increases as we use molecules with a higher dielectric constant. Thus, we can say that Sensitivity is directly proportional to dielectric constant.

Figure 10 describes the variation in Subthreshold swing measured in mv/dec with Dielectric Constant of biomolecules. From the figure, we can observe that for lower values of Dielectric constant, the Subthreshold swing is higher and as the Dielectric constant increases, the subthreshold swing decreases and it is theoretically known that Subthreshold swing should be minimized when allowed by the application. Small subthreshold swing means better channel control, e.g., improved Ion/Ioff, which usually means less leakage, and less energy. For subthreshold circuits it also means better performance.

Finally, the comparison of biosensing parameters for different biomolecules are shown in Table 3. It clearly shows a the DNA molecule has better ON state drain current

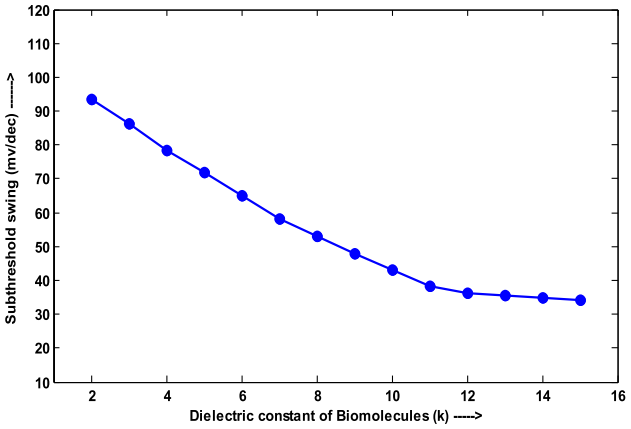

Fig. 10 Subthreshold swing vs Dielectric constant

Table 3 Comparison of biosensing parameters for different Biomolecules

Sl. No	Biomolecules	Ion Current	Sensitivity	Subthreshold swing
1	DNA	8×10^{-8}A	2×10^{8}	51mv/dec
2	Cellulose	5×10^{-8}A	1×10^{7}	64mv/dec
3	APTES	9×10^{-9}A	2×10^{5}	85mv/dec
4	Biotin	4×10^{-9}A	9×10^{3}	82mv/dec
5	Streptavidin	1×10^{-9}A	1×10^{3}	94mv/dec

$(8\times10^{-8}$A) and higher sensitivity (2×10^{8}) which has the higher dielectric constant compare to other molecules. But Streptavidin molecule has high subthreshold swing which has the lower dielectric constant as per available literature.

4 Conclusion

The study and analysis of the biosensor in this paper are done successfully using TFET with nanocavity. Energy band diagram of this device is obtained. Biomolecules consisting of unique dielectrics are placed within the cavity and the difference in I-V graphs are observed which leads us to a conclusion that the dielectric of the material placed has a major impact on I-V characteristics that can be utilized as a biosensor which detects the material that is placed inside the biosensor. The Electric field and Surface Potential characteristics of this biosensor for different biomolecules of varying dielectrics are compared. In addition to this, other conclusions such as I-V characteristic curve (Drain current v/s Gate voltage) is independent of cavity length of this proposed biosensor and on current (Ion) is increased with the increase in dielectric value of the biomolecule is also concluded.

Authors' Contributions Not applicable.

Data Availability Not used any available data.

Code Availability Not used any available code.

Declarations

Ethics Approval Not applicable.

Consent to Participate Not applicable.

Consent for Publication Not applicable.

Conflicts of Interest/Competing Interests There is no conflict of interest.

References

1. Sarkar D, Gossner H, Hansch W, Banerjee K (2013) Impact-ionization field-effect-transistor based biosensors for ultra-sensitive detection of biomolecules. Appl Phys Lett 102:203110
2. Singh R, Kaim S, MedhaShree R et al (2021) Dielectric engineered schottky barrier MOSFET for biosensor applications: proposal and investigation. Silicon. https://doi.org/10.1007/s12633-021-01191-4
3. Vimala P (2018) Charge based quantization model for triple-gate FINFETS. J Nano Electron Phys 10:050151–050155
4. Zhao QT, Rije E, Breuer U, Lenk S, Mantl S (2004) Tuning of silicide Schottky barrier heights by segregation of sulfur atoms. In: 7th International Conference on Solid-State and Integrated Circuits Technology, vol 1, pp 456–459
5. Sumit K, Kondekar PN (2016) Ferroelectric Schottky barrier tunnel FET with gate-drain underlap: Proposal and investigation. Superlattices Microstruct 89:225–230
6. Wangkheirakpam VD, Bhowmick B, Pukhrambam PD (2020) N+ pocket doped vertical TFET based dielectric-modulated biosensor considering non-ideal hybridization issue: a simulation study. IEEE Trans Nanotechnol 19:156–162
7. Reddy NN, Panda DK (2021) A comprehensive review on tunnel field-effect transistor (TFET) based biosensors: recent advances and future prospects on device structure and sensitivity. Silicon 13:3085–3100 (020-00657-1)
8. Singh D, Pandey S, Nigam K, Sharma D, Yadav DS, Kondekar P (2017) A charge-plasma-based dielectric-modulated junctionless TFET for biosensor label-free detection. IEEE Trans Electron Devices 64:271–278
9. Buvaneswari B, Balamurugan NB (2019) 2D analytical modeling and simulation of dual material DG MOSFET for biosensing application. AEU - Int J Electron Commun 99:193–200
10. Im H, Huang XJ, Gu B (2007) A dielectric-modulated field-effect transistor for biosensing. Nat Nanotechnol 2:430–4
11. Latha NKH, Kale S (2020) Dielectric modulated Schottky barrier TFET for the application as label-free biosensor. Silicon 12:2673–2679
12. Kim CH, Jung C, Park HG, Choi YK (2009) Novel dielectric-modulated field-effect transistor for label-free DNA detection. Biochip J 2:127–134
13. Lee C-W, Ferain I, Afzalian A, Yan R (2010) Nima Dehdashti Akhavan, Pedram Razavi, Jean-Pierre Colinge, Performance estimation of junctionless multigate transistors. Solid State Electron 54:97–103
14. Vimala P, Nithin Kumar NR (2019) Comparative Analysis of Various Parameters of Tri-Gate MOSFET with High-K Spacer. JNanoR 56:119–130
15. Kumar MJ, Janardhanan S (2013) Doping-less tunnel field effect transistor: design and investigation. IEEE Trans Electron Devices 60:3285–3290
16. Narang R, Reddy KVS, Saxena M, Gupta RS, Gupta M (2015) A dielectric-modulated tunnel-fet-based biosensor for label-free detection: analytical modeling study and sensitivity analysis. IEEE Trans Electron Devices 59:2809–2817
17. Usha C, Vimala P (2019) An electrostatic analytical modeling of high-k stacked gate-all-around heterojunction tunnel fets considering the depletion regions. AEU-Int J Elec Comm 110:152877
18. Jhaveri R, Nagavarapu V, Woo JCS (2009) Asymmetric Schottky tunneling source SOI MOSFET design for mixed-mode applications. IEEE Trans Electron Devices 56:93–99
19. Narang R, Saxena M, Gupta M (2015) Comparative analysis of dielectric-modulated FET and TFET-based biosensor. IEEE Trans Nanotechnol 14:427–435
20. Gao A, Lu N, Wang Y, Li T (2016) Robust ultrasensitive tunneling- FET biosensor for point-of-care diagnostics. Sci Rep 6:22554
21. Sarkar D, Banerjee K (2012) Proposal for tunnel-field-effect- transistor as ultra-sensitive and label-free biosensors. Appl Phys Lett 100(14):143108
22. Hafiz SA, Iltesha, Ehteshamuddin M, Loan SA (2019) Dielectrically modulated source-engineered charge-plasma-based Schottky-FET as a label-free biosensor. IEEE Trans Electron Devices 66:1905–1910
23. Latha NKH, Kale S (2020) Dielectric modulated schottky barrier TFET for the application as label-free biosensor. Silicon 12:2673–2679. https://doi.org/10.1007/s12633-019-00363-7